

# Synthesis and Photophysics of Silicon Phthalocyanine–Perylenebisimide Triads Connected through Rigid and Flexible Bridges

F. Javier Céspedes-Guirao,<sup>[a]</sup> Luis Martín-Gomis,<sup>[a]</sup> Kei Ohkubo,<sup>[b]</sup>  
Shunichi Fukuzumi,<sup>\*[b, c]</sup> Fernando Fernández-Lázaro,<sup>\*[a]</sup> and Ángela Sastre-Santos<sup>\*[a]</sup>

Dedicated to Prof. Dr. Dr. h.c. Michael Hanack on the occasion of his 80th birthday

**Abstract:** Three new bisperylenebisimide–silicon phthalocyanine triads [(PBI)<sub>2</sub>–SiPcs **1**, **2**, and **3**] connected with either rigid or flexible bridges were synthesized and characterized. A new synthetic approach to connect SiPc and PBI moieties through click chemistry produced triad **3** with an 80% yield. In (PBI)<sub>2</sub>–SiPc **1**, PBI and SiPc are orthogonal and were connected with a rigid connector; triads **2** and **3** bear flexible aliphatic bridges, resulting in a tilted (**2**) or nearly parallel arrangement (**3**) of PBI and SiPc. Photoinduced intramolecular processes in these (PBI)<sub>2</sub>–SiPcs were studied and the results are compared with those of

the reference compounds SiPc-ref and PBI-ref. The occurrence of electron-transfer processes between the SiPc and PBI units was confirmed by time-resolved emission and transient absorption techniques. Charge-separated (CS) states with lifetimes of 0.91, 1.3 and 2.0 ns for triads **1**, **2**, and **3**, respectively, were detected using femtosecond laser flash photolysis. Upon the addition of Mg(ClO<sub>4</sub>)<sub>2</sub>, an increase in the

lifetime of the CS states to 59, 110 and 200 μs was observed for triads (PBI)<sub>2</sub>–SiPcs **1**, **2**, and **3**, respectively. The energy of the CS state (SiPc<sup>+</sup>–PDI<sup>-</sup>/Mg<sup>2+</sup>) is lower than the energy of both silicon phthalocyanine (<sup>3</sup>SiPc<sup>\*</sup>–PDI) and perylenebisimide (SiPc–<sup>3</sup>PDI<sup>\*</sup>) triplet excited states, which decelerates the metal ion-decoupled electron-transfer process for charge recombination to the ground state, thus increasing the lifetime of the CS state. The photophysics of the three triads demonstrate the importance of the rigidity of the spacer and the orientation between donor and acceptor units.

**Keywords:** click chemistry · perylenebisimide · photoinduced electron transfer · photophysics · silicon phthalocyanine

## Introduction

The art of designing and constructing molecular architectures in the search for a controlled transfer of energy and/or electrons has been developed by smart selection from a relatively small number of building blocks,<sup>[1]</sup> thus leading to a deeper knowledge of the photophysical insights, which is of

interest for photochemical energy conversion and storage<sup>[2]</sup> and for the construction of optoelectronic devices.<sup>[3]</sup> In these cases, not only the selection of the building block matters,<sup>[4]</sup> but also the distance,<sup>[5]</sup> the electronic coupling mediated by the connecting unit,<sup>[6]</sup> the solvent polarity,<sup>[7]</sup> and the aggregation status<sup>[8]</sup> can play an important role. Over the years, we have been working with different electron-poor moieties,<sup>[9]</sup> especially with perylenebisimide (PBI), owing to its strong absorption in the 450–600 nm region, its chemical and thermal stabilities, and its ease of chemical modification.<sup>[10,11]</sup> For this study, and in order to increase the electron affinity, we have selected the 1,6,7,12-tetrachloro-substituted PBI (Cl<sub>4</sub>PBI).

As the electron-rich counterpart we use phthalocyanines (Pcs),<sup>[12]</sup> which are the synthetic analogues of naturally occurring porphyrins. Phthalocyanines have excellent light-harvesting abilities, at wavelengths at which the maximum of the solar photon flux occurs, and are also chemically and thermally stable. Among the phthalocyanines, zinc Pcs<sup>[11,13]</sup> have been extensively investigated, because of their long-lived and low-lying triplet excited states, which are of great interest for use in energy-transfer systems, such as in photodynamic therapy (PDT) for cancer treatment.<sup>[14]</sup> Silicon Pcs also attract increasing interest because of their low tendency to aggregate, which accounts for their high solubilities and

[a] F. J. Céspedes-Guirao, Dr. L. Martín-Gomis,  
Prof. Dr. F. Fernández-Lázaro, Prof. Dr. Á. Sastre-Santos  
División de Química Orgánica Instituto de Bioingeniería  
Universidad Miguel Hernández, Elche 03202 (Spain)  
Fax: (+34) 966658351  
E-mail: fdofdez@umh.es  
asastre@umh.es

[b] Dr. K. Ohkubo, Prof. Dr. S. Fukuzumi  
Department of Material and Life Science  
Graduate School of Engineering  
Osaka University and ALCA (JST)  
2-1 Yamada-oka, Suita, Osaka 565-0871 (Japan)  
Fax: (+81) 6-6879-7370  
E-mail: fukuzumi@chem.eng.osaka-u.ac.jp

[c] Prof. Dr. S. Fukuzumi  
Department of Bioinspired Science  
Ewha Womans University, Seoul, 120-750 (Korea)

 Supporting information for this article is available on the WWW under <http://dx.doi.org/10.1002/chem.201100320>.

better photophysical properties (e.g., longer fluorescence lifetimes), and the ease of chemical modification at the axial positions.<sup>[15]</sup> SiPcs are one of the most promising classes of Pc-based photosensitizers for PDT.<sup>[16,17]</sup> Recently, it has been demonstrated that the use of bis(trihexylsilyl oxide)silicon-phthalocyanine and bis(trihexylsilyl oxide) silicon-naphthalocyanine as near-IR dyes in multicolored dye-sensitized polymer/fullerene solar cells, enhances the power conversion efficiency up to 4.3% compared to individual ternary blend solar cells with a single dye. This behavior is probably due to the fact that both dye molecules are located at the interface where no unfavorable aggregation occurs.<sup>[18]</sup> Despite all of these special characteristics, SiPcs have hardly been explored as donor compounds in photoinduced electron-transfer processes.

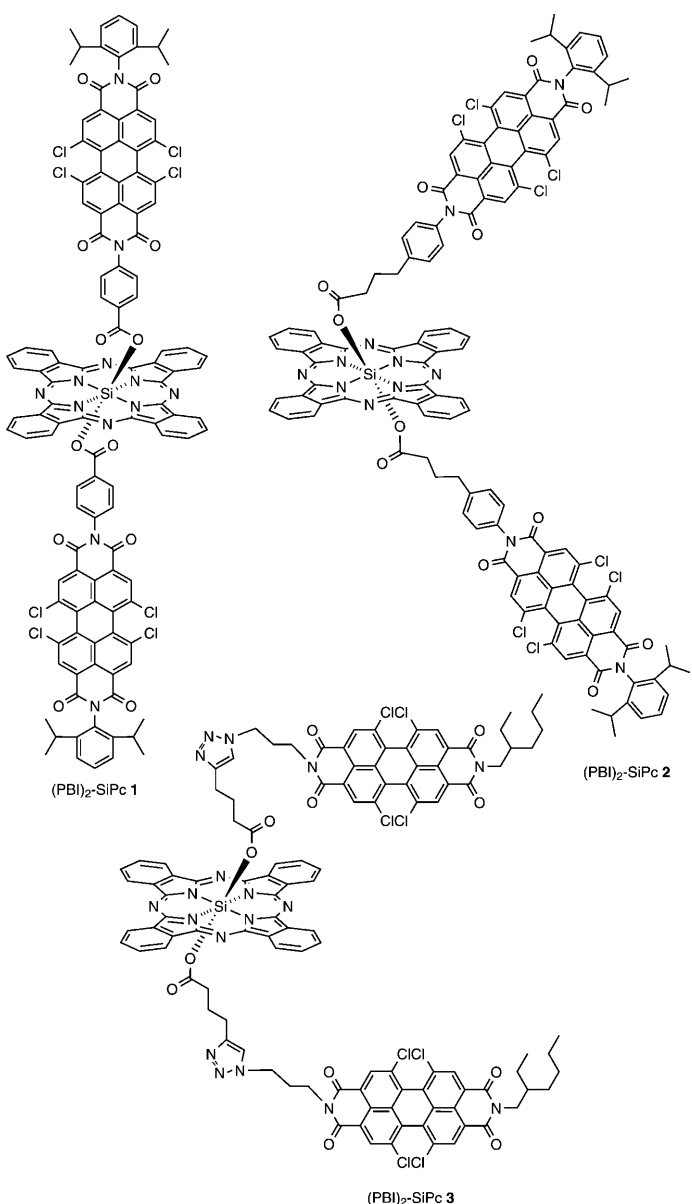
For the purpose of this study, we axially link two  $\text{Cl}_4\text{PBI}$  electron-demanding units to a SiPc. This combination leads to strong light absorption over the whole visible spectrum, while allowing selective excitation of the desired subunits, as the absorption ranges for each moiety are separated. This is the first example of a covalently linked axial PBI-Pc system, which can be compared with previously synthesized coordinatively linked axial<sup>[19]</sup> and covalently linked non-axial systems.<sup>[11a–c,20]</sup> Three different connecting units have been selected that vary the orientation and rigidity between the two different moieties, to gain further insight into the role of these issues in the electron-transfer processes.

To date, the synthesis of SiPcs functionalized in the axial positions has been mainly carried out by nucleophilic displacement of chlorine atoms by hydroxy or carboxy substituted moieties, resulting in compounds with low to moderate yields.<sup>[15]</sup> In this paper we have developed a new strategy to connect SiPcs with PBI units in high yields using click chemistry.

We report herein the synthesis and photophysics of three new  $(\text{PBI})_2\text{-SiPc}$  triads **1–3**.  $(\text{PBI})_2\text{-SiPc}$  triad **1** is connected through a rigid benzene ring in such a way that the PBI and the SiPc are orthogonal, while triads **2** and **3** bear flexible aliphatic bridges. In the case of  $(\text{PBI})_2\text{-SiPc}$  **2** both units are connected through a flexible linker that allows a tilted orientation, while in  $(\text{PBI})_2\text{-SiPc}$  **3**, the PBI and the SiPc moieties are connected by means of a Huisgen reaction where the 1,3-substitution in the triazole ring allows a nearly parallel orientation between both moieties. To the best of our knowledge, this is the first time that a SiPc has been functionalized using a click chemistry reaction which opens a new way for the functionalization of SiPcs.

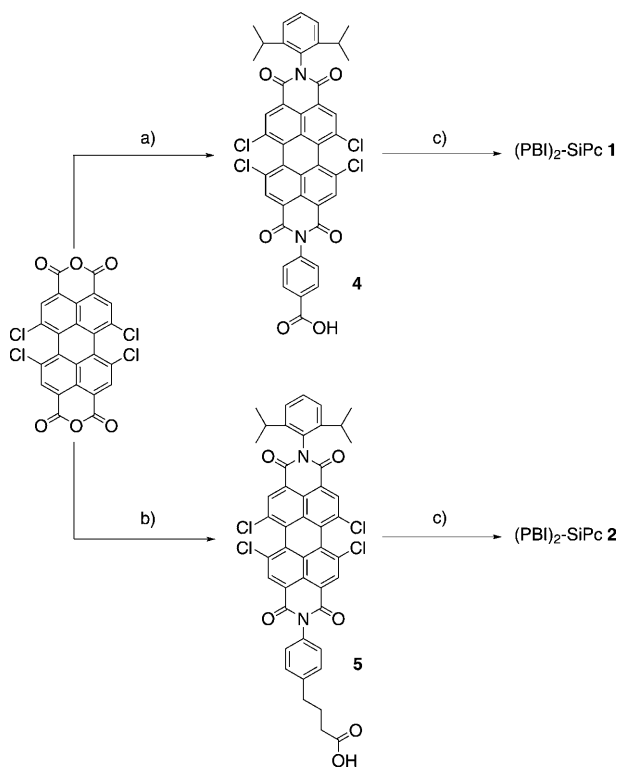
## Results and Discussion

**Synthesis:** The synthesis of triads **1–3** was accomplished using different strategies. A conventional approach to the axial functionalization of dichlorosilicon phthalocyanine compounds was used for triads **1** and **2** (Scheme 1). First we prepared the asymmetrically substituted carboxylic acid PBI derivatives **4** and **5**<sup>[21]</sup> by a one-step statistical condensation

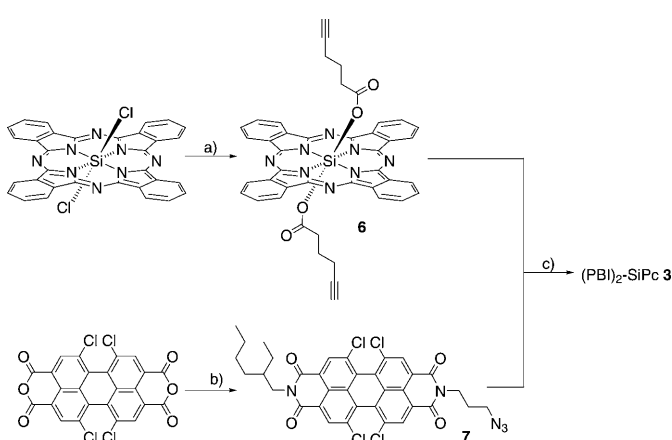


between the tetrachloroperylene bisanhydride and equimolar quantities of the corresponding aniline compounds. Then, nucleophilic displacement of the two chlorine atoms from the dichlorosilicon phthalocyanine afforded  $(\text{PBI})_2\text{-SiPc}$  triads **1** and **2** in 5 and 15% yields, respectively.

The synthesis of  $(\text{PBI})_2\text{-SiPc}$  triad **3** relied on a well-known click reaction, namely the copper-catalyzed [3+2] Huisgen cycloaddition reaction between the alkyne **6** and azide **7** (Scheme 2). The best results were obtained using 10% mol of sodium ascorbate and 5% of  $\text{CuSO}_4 \cdot 5\text{H}_2\text{O}$  in a 4:1 THF:H<sub>2</sub>O mixture, and heating at 60°C for 24 h. Under these conditions, the desired  $(\text{PBI})_2\text{-SiPc}$  triad **3** was obtained in 80% yield. SiPc **6** was obtained by reaction of the SiPcCl<sub>2</sub> with 5-hexynoic acid in 30% yield. PBI **7** was afforded by condensation of 3-azidopropylamine and 2-ethylhexylamine with tetrachloroperylene bisanhydride, in 35% yield.



Scheme 1. Synthesis of  $(\text{PBI})_2\text{-SiPc}$  triads **1** and **2**. a) 4-Aminobenzoic acid, 2,6-diisopropylaniline, propionic acid, 140°C. b) 4-(4-Aminophenyl)butyric acid, 2,6-diisopropylaniline, propionic acid, 140°C. c) Dichlorosilicon phthalocyanine, dyglime, 160°C.



Scheme 2. Synthesis of  $(\text{PBI})_2\text{-SiPc}$  triad **3**. a) 5-Hexynoic acid, dyglime, 160°C. b) 3-Azidopropylamine, 2-ethylhexylamine, toluene, 110°C. c) Copper(II) sulfate pentahydrate, sodium ascorbate, tetrahydrofuran,  $\text{H}_2\text{O}$ , 60°C.

All new compounds were characterized by  $^1\text{H}$  NMR, UV/Vis, and FT-IR spectroscopies, mass spectrometry, and elemental analysis. The good resolution of the  $^1\text{H}$  NMR spectra of  $(\text{PBI})_2\text{-SiPc}$  triads **1–3** registered in deuterated chloroform clearly indicates the lack of aggregation phenomena in solution, mainly due to the presence of the bulky perylenebisimide moieties in the axial positions of the phthalocya-

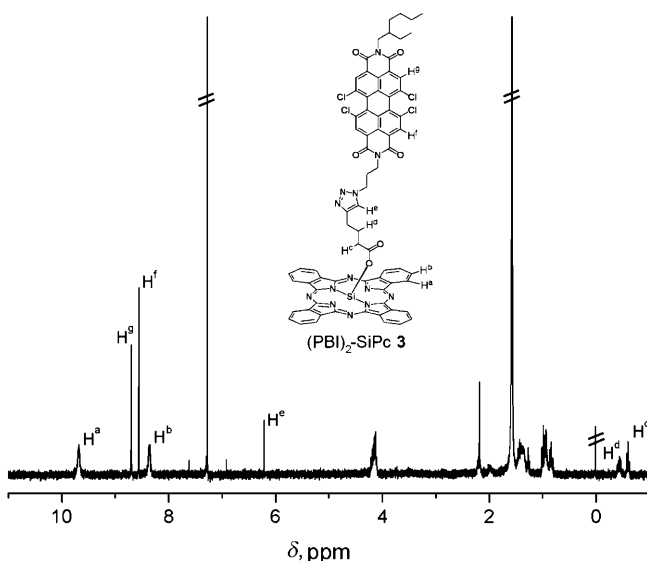


Figure 1.  $^1\text{H}$  NMR spectrum ( $\text{CDCl}_3$ , 300 MHz, 25°C) of  $(\text{PBI})_2\text{-SiPc}$  triad **3**.

nine ring. Figure 1 shows, as an example, the  $^1\text{H}$  NMR spectrum of  $(\text{PBI})_2\text{-SiPc}$  triad **3** in deuterated chloroform. The peaks corresponding to the two different sets of aromatic protons of the phthalocyanine are located around 9.6–9.7 and 8.3–8.4 ppm, while the peaks corresponding to the protons of the perylenebisimide moiety are centered at 8.69 and 8.55 ppm. The integration of these signals, together with the characteristic singlet of the triazole linker (6.20 ppm), clearly indicate the success in the coupling between the alkyne-substituted silicon phthalocyanine **6** and the azide-substituted tetrachloroperylene **7** through a click reaction.

**Spectroscopic and redox properties:** Figure 2 shows the comparison of the absorption spectra of  $(\text{PBI})_2\text{-SiPc}$  triads **1–3** with SiPc and PBI reference compounds **6** and **7**. We can clearly see a set of absorption bands between 486 and 520 nm, corresponding to the PBI moiety, and a sharp Q band, centered at 685 nm, characteristic of non-aggregated phthalocyanine compounds. A decrease in the extinction coefficient of the phthalocyanine Q-band is observed for triads

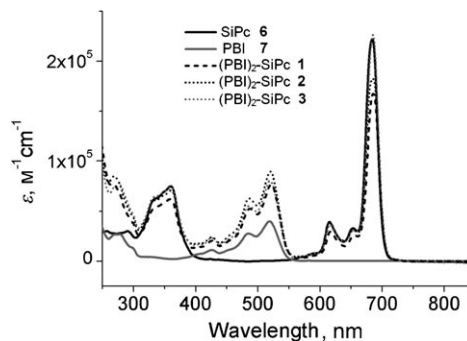


Figure 2. UV/Vis spectra in  $\text{CHCl}_3$  of SiPc **6**, PBI **7** and  $(\text{PBI})_2\text{-SiPc}$  **1–3** triads.

**1** and **2**, but not for triad **3**. This effect could be explained by a possible  $\pi$ - $\pi$  interaction between the PBI units and the phthalocyanine core as a consequence of the close distance of both moieties; this interaction decreases as the length of the linker between the electroactive units becomes longer. Taking this into account, the absorption spectra of triads **1–3** can be considered as a reasonable superposition of the absorption spectrum of each component, which indicates a weak, or nonexistent, electronic interaction between the electroactive chromophores in the ground state.

The cyclic voltammograms in benzonitrile (PhCN) of  $(\text{PBI})_2\text{-SiPc}$  triads **1–3**, together with those of the reference compounds, SiPc **6** and PBI **7**, are shown in Figure 3. From the shape of the voltammograms and the calculated reduction and oxidation potential values, we infer that the electronic interaction between the electroactive moieties is very weak for all compounds. Only in triad **1**, which has the shortest linker of all the studied compounds, the interaction could be slightly more intense due to the rigid nature of the aromatic linker and the close distance between electroactive moieties as previously detected by UV/Vis spectroscopy. In all cases the one-electron oxidation and reduction waves are virtually the superposition of those of the unlinked PBI and

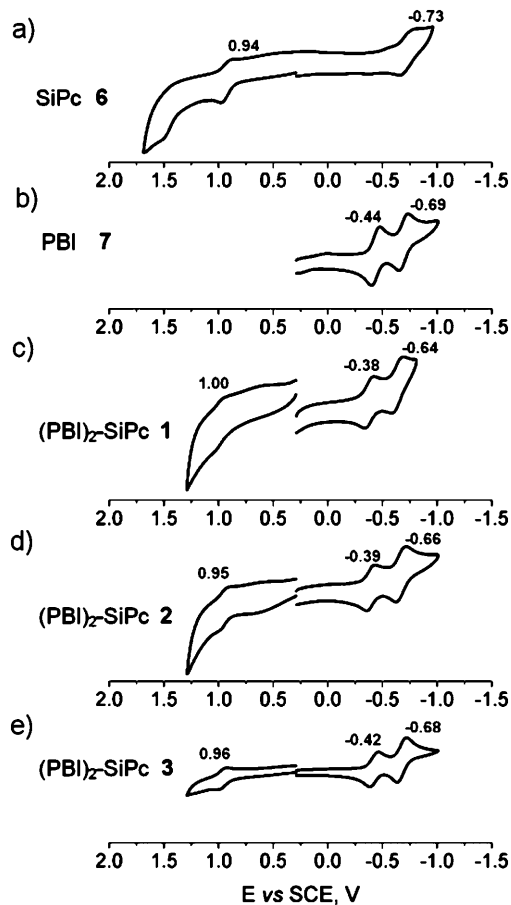


Figure 3. Cyclic voltammograms of a) SiPc **6**, b) PBI **7**, c)  $(\text{PBI})_2\text{-SiPc}$  triad **1**, d)  $(\text{PBI})_2\text{-SiPc}$  triad **2** and e)  $(\text{PBI})_2\text{-SiPc}$  triad **3**, in deaerated PhCN containing 0.10 M  $\text{Bu}_4\text{NPF}_6$ .

SiPc units, confirming the lack of electronic interaction between the electroactive moieties in the ground state, as already observed in the absorption spectra.

**Theoretical calculations:** HOMO and LUMO orbitals of  $(\text{PBI})_2\text{-SiPc}$  triads **1–3** calculated with the optimized structure using the DFT method<sup>[22]</sup> are shown in Figure 4. The results indicate that the HOMO is localized on the SiPc moiety, the LUMO is on one PDI moiety, and the LUMO+1 is localized on the other PDI moiety.

**Photoinduced charge separation:** The photophysical behavior of triads **1–3** was qualitatively investigated in PhCN by steady-state fluorescence using 361 and 522 nm light excitation, which selectively excites the SiPc and PDI entities, respectively. As shown in Figure 5, the fluorescence spectrum of SiPc reference **6** exhibits an emission band centered at

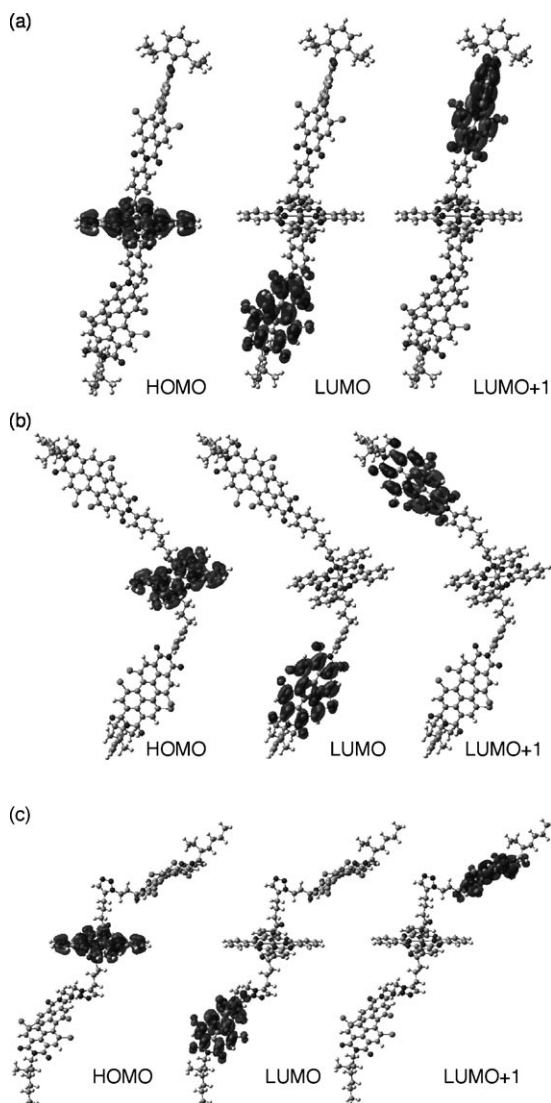


Figure 4. HOMO, LUMO and LUMO+1 of a)  $(\text{PBI})_2\text{-SiPc}$  triad **1**, b)  $(\text{PBI})_2\text{-SiPc}$  triad **2** and c)  $(\text{PBI})_2\text{-SiPc}$  triad **3**, calculated using DFT at the B3LYP/3-21G level.

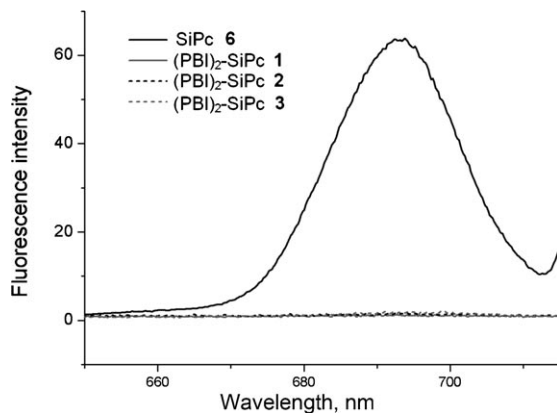


Figure 5. Fluorescence spectra of SiPc **6** and (PBI)<sub>2</sub>-SiPc **1–3** in deaerated PhCN. Excitation wavelength = 361 nm.

693 nm (1.79 eV). The axial linkage with the PBI units efficiently quenches this emission band (Figure 5) suggesting a non-radiative deactivation of the singlet excited state of SiPc (<sup>1</sup>SiPc\*; \* denotes the excited state) according to previously reported data for singlet excited state values of PBI and SiPc units.<sup>[15]</sup> The quenching rate constant for (PBI)<sub>2</sub>-SiPc triads **1–3** is  $>5 \times 10^{10} \text{ s}^{-1}$  from the efficient fluorescence quenching (>99 %) and the fluorescence lifetime of SiPc **6** (8.5 ns) (see Supporting Information Figure S1). The intensity of the <sup>1</sup>PBI\* emission, centered at 550 nm (2.25 eV) after 522 nm light excitation (selective excitation of the PBI unit), dramatically decreases for triads **1–3**, compared to the emission intensity observed by exciting the PBI reference compound **7** (Figure 6). Such fluorescence quenching in a polar solvent suggests either an energy- or electron-transfer process.

Interestingly, in the case of triad **1**, a concomitant appearance of a fluorescence emission band can be distinguished in the area where the <sup>1</sup>SiPc\* emission maximum appears (Figure 6, inset). The appearance of this fluorescence emission band assigned to <sup>1</sup>SiPc\*, together with its weak intensi-

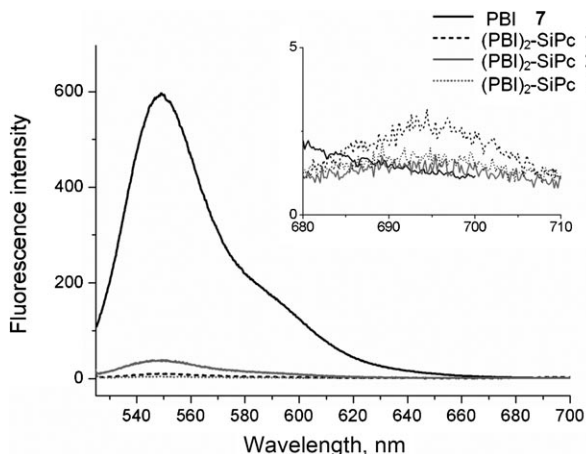


Figure 6. Fluorescence spectra of PBI **7** and (PBI)<sub>2</sub>-SiPc **1–3** in deaerated PhCN. Excitation wavelength = 522 nm.

ty, suggests that the deactivation of <sup>1</sup>PBI\* occurs through a non-radiative process as well, but its first step involves energy transfer from the perylenebisimide to the phthalocyanine unit. Photoinduced electron transfer was examined by femtosecond laser flash photolysis measurements. Figure 7 shows that 430 nm excitation of PBI **7** with a femtosecond laser pulse yields a transient with absorptions at 830 nm and 980 nm which corresponds to the singlet excited state <sup>1</sup>PBI\*.

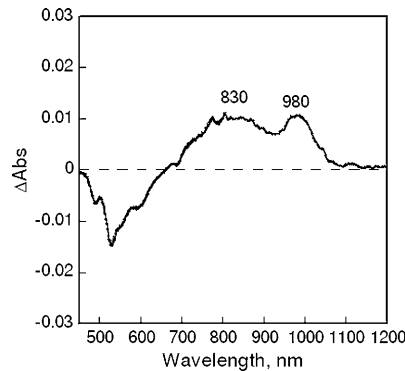


Figure 7. Femtosecond transient absorption spectrum of PBI **7** in deaerated PhCN taken at 10 ps after 430 nm laser excitation.

The behavior of the (PBI)<sub>2</sub>-SiPc triads **1–3** is similar (Figures 8–10) to that of PBI **7**. Thus, photoexcitation of a deaerated PhCN solution containing (PBI)<sub>2</sub>-SiPc **1** with 430 nm excitation affords, initially, the singlet excited state of the perylene moiety, as indicated by the broad absorptions centered at 830 and 980 nm (see Figure 8a). These absorptions slowly vanish, leaving sharper peaks at 580 and 850 nm, which are indicative of the presence of the SiPc<sup>+</sup> radical cation.<sup>[15d,e,h,23]</sup> The broad absorption around 980 nm obscures the detection of the SiPc singlet excited state, which should absorb at 950 nm;<sup>[15h]</sup> however, the fluorescence quenching results for triad **1** and our previous experience<sup>[15]</sup> support its formation. Thus, the transient absorption spectra in Figures 8–10 clearly indicate the formation of the CS state [PBI-SiPc<sup>+</sup>-PBI<sup>-</sup>], in which one of the two PBI units becomes the radical anion by electron transfer from <sup>1</sup>SiPc\* to PBI in the triads.

The energy-transfer rate constant from <sup>1</sup>PBI\* to <sup>1</sup>SiPc\* was determined from the decay of the band at 980 nm for triads **1–3**. Rate constants of  $6.0 \times 10^{10} \text{ s}^{-1}$  for (PBI)<sub>2</sub>-SiPc triad **1**,  $1.0 \times 10^{11} \text{ s}^{-1}$  for (PBI)<sub>2</sub>-SiPc triad **2**, and  $1.2 \times 10^{11} \text{ s}^{-1}$  for (PBI)<sub>2</sub>-SiPc triad **3** were determined, with lifetimes of 17, 10 and 8.3 ps, respectively (Figures 8b–10b). These data are in accordance with the fluorescence quenching results. The results indicate that the compounds with flexible spacers, which allow a non-perpendicular orientation between the SiPc and the PDI moieties (**2**, **3**), afford faster energy-transfer rate constants ( $1.0\text{--}1.2 \times 10^{11} \text{ s}^{-1}$ ).

The formation and decay profiles of the CS state of SiPc triad **1** are different from those of triads **2** and **3**. The rate constants of formation and decay of the CS state of (PBI)<sub>2</sub>-

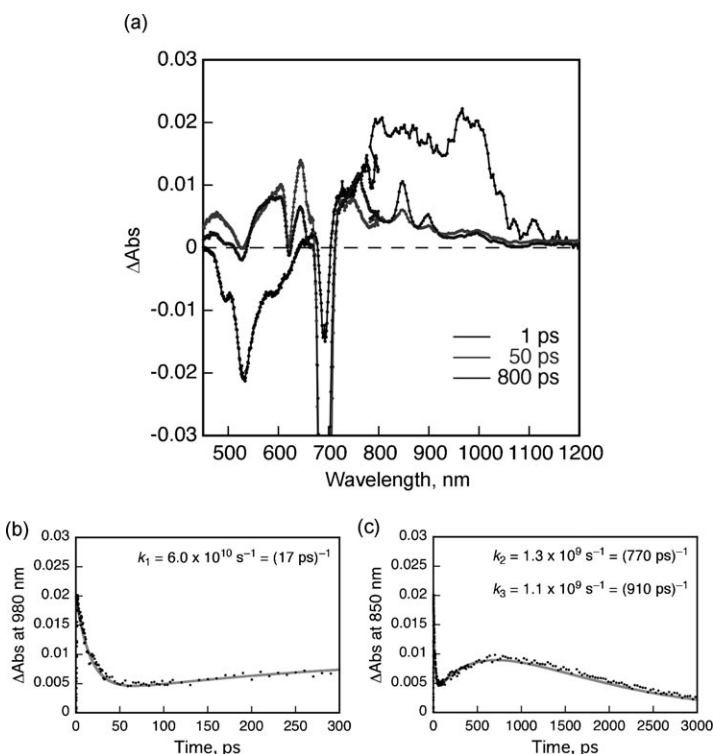


Figure 8. a) Femtosecond transient absorption spectra of  $(\text{PBI})_2\text{-SiPc}$  **1** in de-aerated PhCN at 298 K after 430 nm laser excitation. b) Time profile of absorbance at 980 nm. c) Time profile of absorbance at 850 nm. Gray lines represent a tri-exponential fit.

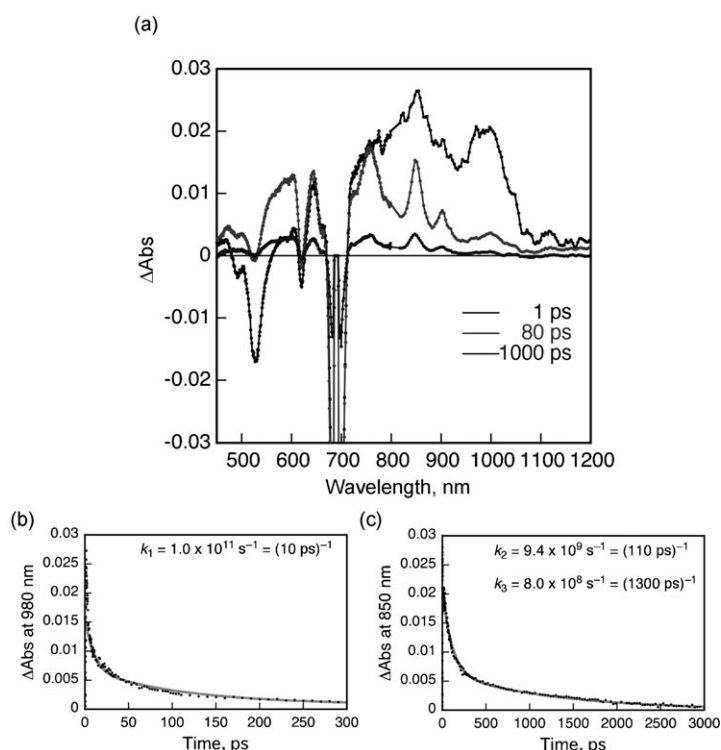


Figure 9. a) Femtosecond transient absorption spectra of  $(\text{PBI})_2\text{-SiPc}$  **2** in de-aerated PhCN at 298 K after 430 nm laser excitation. b) Time profile of absorbance at 980 nm. c) Time profile of absorbance at 850 nm. Gray lines represent a tri-exponential fit.

SiPc **1**, determined from the rise and decay of the absorbance at 850 nm (Figure 8c), are  $1.3 \times 10^9$  and  $1.1 \times 10^9 \text{ s}^{-1}$ , respectively, leading to a CS lifetime of 0.91 ns. The absorbance decays of  $(\text{PBI})_2\text{-SiPc}$  triads **2** and **3** are fitted to tri-exponential functions, as shown in Figures 9c and 10c, respectively. From the fast decay component in the absorbance at 850 nm, due to  $\text{SiPc}^+$ , the rate constants of formation of the CS state for triads **2** and **3** were determined to be  $9.4 \times 10^9$  and  $5.7 \times 10^9 \text{ s}^{-1}$  respectively, which is in agreement with the value determined from the fluorescence quenching of  ${}^1\text{SiPc}^*$  ( $> 5 \times 10^{10} \text{ s}^{-1}$ ). The lifetimes of the CS state in PhCN for triads **2** and **3** are 1.3 and 2.0 ns respectively, obtained from the slow component of the absorbance decay at 850 nm.

The presence of a flexible linker in the  $(\text{PBI})_2\text{-SiPc}$  triads, together with a tilted orientation of the PDI units versus the SiPc, affords high electron-transfer rate constants to generate the CS state, but low recombination rate constants. Hence the CS lifetime is the longest in triad **3** (2.1 ns), followed by triad **2**, (1.3 ns) and then triad **1** (0.9 ns).

The results of nanosecond laser flash photolysis with photoexcitation at 355 nm indicate that the same photo-physical decay pathways are followed in the three  $(\text{PBI})_2\text{-SiPc}$  triads. As shown in Figure 11a for triad **3**, the absorption bands at 530 and 760 nm corresponding to the triplet excited states,  ${}^3\text{SiPc}^*$  and  ${}^3\text{PBI}^*$ , respectively, are detected at 10  $\mu$ s after laser excitation. The decay of  ${}^3\text{SiPc}^*$  at 530 nm is significantly faster than that of  ${}^3\text{PBI}^*$ . The transient absorption band of  ${}^3\text{PBI}^*$  remains at 70  $\mu$ s (grey plot in Figure 11a). From the decay of the band of  ${}^3\text{SiPc}^*$  (for triad **3** see Figure 11b) the lifetime of the  $(\text{PBI})_2\text{-}{}^3\text{SiPc}^*$  species for triads **1–3** are determined to be 50, 51 and 100  $\mu$ s, respectively (see Supporting Information Figures S2 and S3 for triads **1** and **2**, respectively). This decay process is assigned to the energy transfer from  ${}^3\text{SiPc}^*$  to PBI forming  $\text{SiPc-}{}^3\text{PBI}^*$ .

Nanosecond laser flash photolysis with photoexcitation at 355 nm, of  $(\text{PBI})_2\text{-SiPc}$  triads **1–3** in PhCN after the addition of magnesium perchlorate  $[\text{Mg}(\text{ClO}_4)_2]$ , yielded quite different results from the previous ones. As shown in Figure 12a for  $(\text{PBI})_2\text{-SiPc}$  triad **3**, the bands observed at 580 and 850 (SiPc $^+$ ) confirm the formation of the CS state. From the decay of the bands at 850 nm the CS-state lifetimes are calculated to be 59, 110 and 210  $\mu$ s for  $(\text{PBI})_2\text{-SiPc}$  triads **1–3**, respectively (see Figure 12b for triad **3** and Supporting Information Figures S4 and S5 for triads **1** and **2**, respectively). Again, the longer lived CS state corresponds to the  $(\text{PBI})_2\text{-SiPc}$  triad **3**, confirming that the quasi-parallel location of the two moieties through a non-rigid linker hinders the back electron-transfer process. According to the literature,<sup>[15d,e,h]</sup> the energy of the triplet excited state of SiPc is 1.26 eV. The CS-state energy for  $(\text{PBI})_2\text{-SiPc}$  **3** (1.38 eV), determined from  $E_{\text{ox}}$  of SiPc (0.96 V vs. SCE) and  $E_{\text{red}}$  of PBI (-0.42 V vs. SCE), is higher than the energy of the triplet excited state of SiPc [ ${}^3\text{SiPc}^*-(\text{PBI})_2$ ]. The triplet excited-

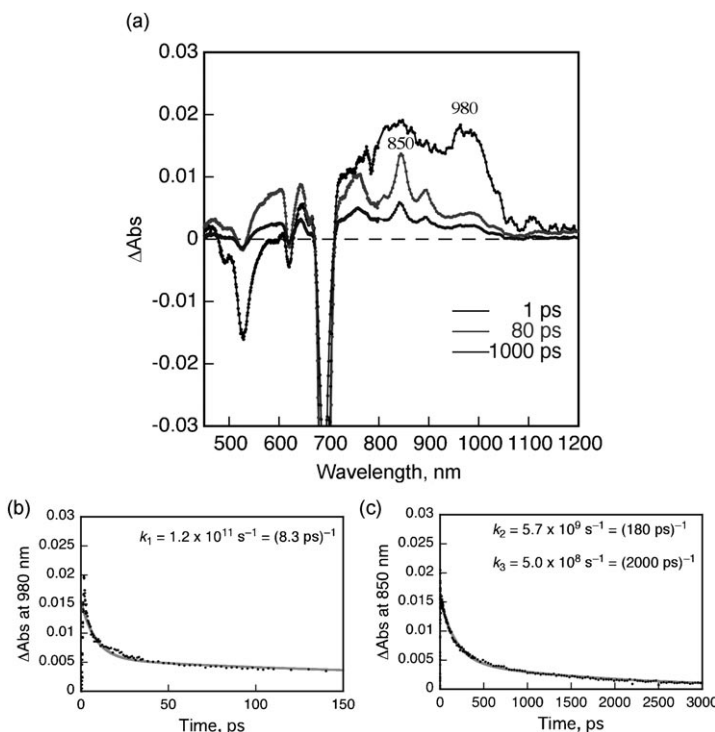


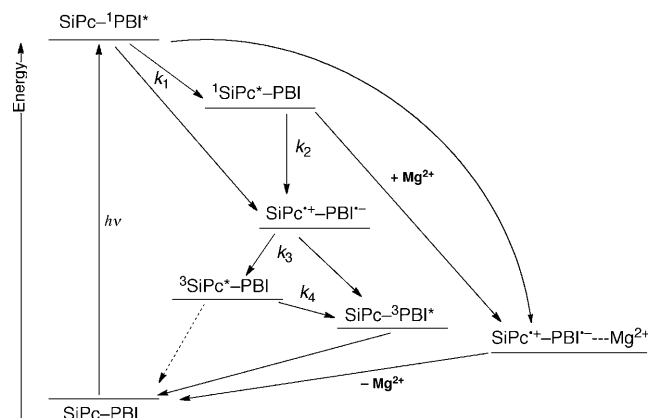
Figure 10. a) Femtosecond transient absorption spectra of  $(\text{PBI})_2\text{-SiPc } \mathbf{3}$  in deaerated PhCN at 298 K after 430 nm laser excitation. b) Time profile of absorbance at 980 nm. c) Time profile of absorbance at 850 nm. Gray lines represent a tri-exponential fit.

state energy of PBI ( $\text{PBI-SiPc}^-\text{-}{}^3\text{PBI}^*$ , 1.07 eV)<sup>[24]</sup> is also lower than the energy of the CS state. The CS-state energies for  $(\text{PBI})_2\text{-SiPc } \mathbf{1}$  (1.38 eV) and  $(\text{PBI})_2\text{-SiPc } \mathbf{2}$  (1.34 eV) are also higher in energy than  ${}^3\text{SiPc}^*\text{-}(\text{PBI})_2$  and  $\text{PBI-SiPc}^-\text{-}{}^3\text{PBI}^*$ . In the presence of magnesium ions, however, the one-electron reduction potential of PBI is shifted from  $-0.44$  V versus SCE to  $+0.14$  V (Figure 13).

The energy of the CS state ( $\text{PBI-SiPc}^+\text{-PBI}^-\text{/Mg}^{2+}$ ) is 0.81 eV, which is now lower than the energy of the SiPc triplet excited state, and results in the deceleration of the metal ion-decoupled back electron transfer to the ground state which increases the lifetime of the CS state.<sup>[1b]</sup>

Scheme 3 summarizes the energy diagram of the photoinduced events in  $(\text{PBI})_2\text{-SiPc } \mathbf{1}\text{-}\mathbf{3}$  triads, in which one acceptor unit is omitted for clarity. In each case, energy transfer occurs from the  ${}^1\text{PBI}^*$  to the  ${}^1\text{SiPc}^*$ , followed by photoinduced electron transfer from the  ${}^1\text{SiPc}^*$  unit to the acceptor moiety to produce the CS state. There are three pathways for the charge recombination (CR): CR to  ${}^3\text{PBI}^*$ , CR to  ${}^3\text{SiPc}^*$ , and CR to the ground state. The third pathway is unlikely to occur because, as previously described, the decay of the CS state affords the phthalocyanine triplet excited state  ${}^3\text{SiPc}^*$ .<sup>[15e]</sup>

The rate constants and CS state lifetimes for the  $(\text{PBI})_2\text{-SiPc}$  triads are listed in Table 1. According to the data, the back electron transfer for triad **3** is slower as a consequence of the flexible linker and the orientation of the two electroactive subunits.



Scheme 3. Energy diagram for  $(\text{PBI})_2\text{-SiPc}$  triads **1-3**.

## Conclusion

We have synthesized, for the first time, triad systems based on SiPc and PBI building blocks. A new strategy using click chemistry has been developed to connect SiPc and PBI in triad **3** in a high yield (80%). This strategy opens a new route to the functionalization of SiPc. The

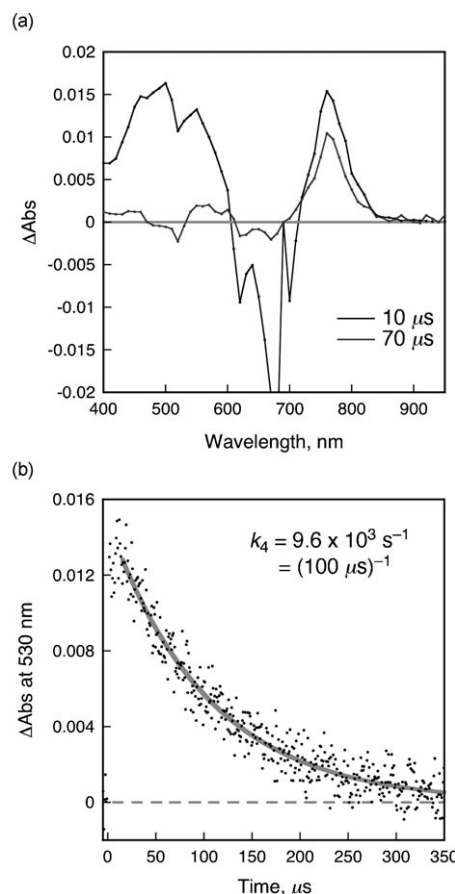


Figure 11. a) Nanosecond transient absorption spectra of  $(\text{PBI})_2\text{-SiPc } \mathbf{3}$  in deaerated PhCN at 298 K after 355 nm laser excitation. b) Time profile of absorbance at 530 nm. Gray line represents a mono-exponential fit.

Table 1. Rate constants of singlet energy transfer ( $k_1$ ), electron transfer ( $k_2$ ), back electron transfer ( $k_3$ ) and triplet energy transfer of  $(\text{PBI})_2\text{-SiPc}$  triads **1–3** and CS lifetimes ( $\tau$ ) with and without  $\text{Mg}^{2+}$ .

	$(\text{PBI})_2\text{-SiPc}$ <b>1</b>	$(\text{PBI})_2\text{-SiPc}$ <b>2</b>	$(\text{PBI})_2\text{-SiPc}$ <b>3</b>
$k_1 [\text{s}^{-1}]$	$6.0 \times 10^{10}$	$1.0 \times 10^{11}$	$1.2 \times 10^{11}$
$k_2 [\text{s}^{-1}]$	$1.3 \times 10^9$	$9.4 \times 10^9$	$5.7 \times 10^9$
$k_3 [\text{s}^{-1}]$	$1.1 \times 10^9$	$8.0 \times 10^8$	$5.0 \times 10^8$
$k_4 [\text{s}^{-1}]$	$2.0 \times 10^4$	$2.0 \times 10^4$	$9.6 \times 10^3$
$\tau(\text{CS}) [\text{ns}]$	0.9	1.3	2.0
$\tau(\text{CS}) \text{ with } \text{Mg}^{2+} [\mu\text{s}]$	59	110	210

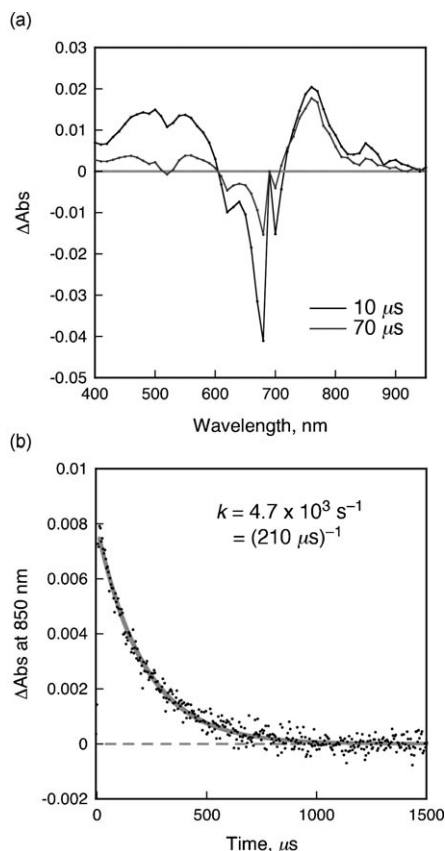


Figure 12. a) Nanosecond transient absorption spectra of  $(\text{PBI})_2\text{-SiPc}$  **3** in deaerated PhCN containing 10 mM  $\text{Mg}(\text{ClO}_4)_2$  at 298 K after 355 nm laser excitation. b) Time profile of absorbance at 850 nm. Gray line represents a mono-exponential fit.

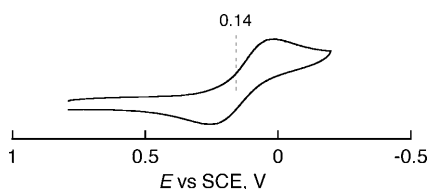


Figure 13. Cyclic voltammogram of PBI **7** (1.0 mM) in the presence of  $\text{Mg}(\text{ClO}_4)_2$  (10 mM) in deaerated PhCN at 298 K. Sweep rate:  $0.1 \text{ Vs}^{-1}$ .

photoinduced electron-transfer processes between SiPc and the PBI were measured by time-resolved emission and transient absorption techniques. By using femtosecond laser flash photolysis, the CS lifetimes of the triads  $(\text{PBI})_2\text{-SiPc}$  **1–3** were determined to be 0.91, 1.3, and 2.0 ns, respectively.

Upon the addition of  $\text{Mg}(\text{ClO}_4)_2$ , an increase in the CS lifetimes of **1**, **2**, and **3** was observed, with values of 59, 110, and 210  $\mu\text{s}$ , respectively. The energy of the CS state  $(\text{PBI}-\text{SiPc}^{\cdot+}-\text{PBI}^{\cdot-}/\text{Mg}^{2+})$  becomes lower than the energy of the silicon phthalocyanine triplet excited state  $(\text{PBI}-{}^3\text{SiPc}^{\ast}-\text{PBI})$ , resulting in deceleration of the metal-ion-decoupled back-electron-transfer process to the ground state, thus increasing the lifetime of the CS state. The photophysics of the three triads demonstrate the importance in photoinduced events of the rigidity of the spacer and the orientation between donor and acceptor units.

## Experimental Section

**General:** All chemicals were reagent-grade, purchased from commercial sources, and used as received, unless otherwise specified. Column chromatography was performed using  $\text{SiO}_2$  (40–63  $\mu\text{m}$ ) TLC plates coated with  $\text{SiO}_2$  60F254 and visualized by UV light. NMR spectra were measured with a Bruker AC 300. UV/Vis spectra were recorded with a Helios Gamma spectrophotometer. Fluorescence spectra were recorded with a Perkin-Elmer LS 55 Luminescence Spectrometer and IR spectra with a Nicolet Impact 400D spectrophotometer. Mass spectra were obtained from a Bruker Reflex III matrix-assisted laser desorption/ionization time of flight (MALDI-TOF) and from a VG AutoSpec instrument (FAB). Elemental analyses were performed on a LECO CHNS-932 elemental analyzer.

**PBI derivative 4:** A mixture of 1,6,7,12-tetrachloroperylene-3,4:9,10-tetracarboxylic acid (3 g, 5.66 mmol) and propionic acid (120 mL) was stirred at RT for 15 min, then 2,6-diisopropylaniline (1.01 mg, 5.7 mmol) and 4-aminobenzoic acid (782 mg, 5.7 mmol) were added. The mixture was stirred at 140°C under argon atmosphere for 24 h. After cooling, the crude product was poured over an ice/water mixture, filtered, washed with cold water several times and, finally, purified twice by flash chromatography ( $\text{SiO}_2$ ,  $\text{CH}_2\text{Cl}_2 \rightarrow \text{CH}_2\text{Cl}_2/\text{acetone}$  8:2), to yield an orange solid (690 mg, 24% yield).  $^1\text{H}$  NMR (300 MHz,  $\text{CDCl}_3$ , 25°C, TMS):  $\delta = 8.78$  (s, 2H; 2×H-PBI), 8.77 (s, 2H; 2×H-PBI), 8.35 (d,  $J = 8.5 \text{ Hz}$ , 2H; 2×H-Ar), 7.52 (t,  $J = 8.1 \text{ Hz}$ , 1H; H-Ar'), 7.48 (d,  $J = 8.5 \text{ Hz}$ , 2H; 2×H-Ar), 7.38 (d,  $J = 8.1 \text{ Hz}$ , 2H; 2×H-Ar'), 2.80–2.68 (m, 2; 2×CH-(CH<sub>3</sub>)<sub>2</sub>), 1.24–1.16 ppm (m, 12H; 4×CH<sub>3</sub>).  $^{13}\text{C}$  NMR (75 MHz,  $\text{CDCl}_3$ , 9:1  $\text{CD}_3\text{CN}$ , 25°C, TMS):  $\delta = 166.4$ , 161.9, 161.8, 145.3, 138.6, 135.2, 135.1, 132.9, 132.8, 131.3, 131.2, 130.7, 130.3, 129.7, 129.5, 128.6, 128.5, 123.8, 123.5, 123.3, 122.9, 122.8, 116.3, 28.8, 23.5 ppm; IR (KBr):  $\tilde{\nu} = 2962$ , 2928, 1715 (C=O acid), 1677 (C=O imide) 1588, 1411, 1382, 1314, 1293, 1240, 1189, 801, 748, 686, 546 cm<sup>-1</sup>; UV/Vis ( $\text{CH}_2\text{Cl}_2$ ):  $\lambda_{\text{max}}$  (log ε) = 231 (4.89), 269 (4.47), 427 (3.96), 487 (4.40), 521 nm (4.56); MS (MALDI-TOF):  $m/z$ : 807 [M+H]<sup>+</sup>; elemental analysis calcd (%) for  $\text{C}_{45}\text{H}_{26}\text{Cl}_4\text{N}_2\text{O}_6\text{H}_2\text{O}$ : C 62.47, H 3.42, N 3.39; found C 62.24, H 3.82, N 3.23.

**(PBI)<sub>2</sub>-SiPc 1:** SiPcCl<sub>2</sub> (40 mg, 0.065 mmol) and PBI **4** (230 mg, 0.28 mmol) in dylime (5 mL) were stirred at 160°C under argon atmosphere for 12 h. After cooling, the crude product was poured over water, filtered, washed with water several times and, finally, purified by flash chromatography ( $\text{SiO}_2$ ,  $\text{CH}_2\text{Cl}_2/\text{acetone}$  20:1 →  $\text{CH}_2\text{Cl}_2/\text{MeOH}$  10:1) to yield a dark green solid (7 mg, 5% yield).  $^1\text{H}$  NMR (300 MHz,  $\text{CDCl}_3$ , 25°C, TMS):  $\delta = 9.80$ –9.76 (m, 8H; 8×H-Pc), 8.68 (s, 4H; 4×H-PBI), 8.45–8.41 (m, 8H; 8×H-Pc), 8.41 (s, 4H; 4×H-PBI), 7.50 (t,  $J = 7.6 \text{ Hz}$ , 2H; 2×H-Ar'), 7.33 (d,  $J = 7.6 \text{ Hz}$ , 4H; 4×H-Ar'), 6.22 (d,  $J = 8.6 \text{ Hz}$ , 4H; 4×H-Ar), 5.39 (d,  $J = 8.6 \text{ Hz}$ , 4H; 4×H-Ar), 2.74–2.61 (m, 4H; 4×CH-(CH<sub>3</sub>)<sub>2</sub>), 1.19–1.12 ppm (m, 24H; 8×CH<sub>3</sub>).  $^{13}\text{C}$  NMR (75 MHz,  $\text{CDCl}_3$ , 25°C, TMS):  $\delta = 162.2$ , 161.5, 158.3, 150.3, 145.5, 136.5, 135.6, 135.5, 135.3, 133.4, 133.3, 133.0, 131.6, 131.5, 131.4, 131.3, 129.8, 128.8, 128.7, 127.4, 126.9, 124.2, 124.1, 123.8, 123.3, 123.1, 122.8, 29.3, 24.0 ppm; IR (KBr):  $\tilde{\nu} = 2961$ , 1716 (C=O acid), 1679 (C=O imide) 1588, 1431, 1380, 1336, 1291, 1240, 1188, 1166, 1123, 1082, 914, 805, 761, 737, 686, 546 cm<sup>-1</sup>; UV/Vis ( $\text{CH}_2\text{Cl}_2$ ):  $\lambda_{\text{max}}$  (log ε) = 232 (5.23), 267 (4.89), 359

(4.79), 427 (4.31), 488 (4.72), 521 (4.88), 617 (4.47), 655 (4.41), 686 nm (5.22); HRMS (MALDI-TOF):  $m/z$ : calcd for  $C_{118}H_{66}Cl_8N_{12}O_{12}Si$ : 2150.2195 [ $M]^+$ ; found: 2150.2209; elemental analysis calcd (%) for  $C_{118}H_{66}Cl_8N_{12}O_{12}Si \cdot 6H_2O$ : C 62.61, H 3.47, N 7.43; found C 62.65, H 3.67, N 6.93.

**PBI derivative 5.**<sup>[21]</sup> A mixture of 1,6,7,12-tetrachloroperylene-3,4:9,10-tetracarboxylic anhydride (3 g, 5.66 mmol) and 100 mL of propionic acid was stirred at RT for 15 min, then 2,6-diisopropylaniline (1 g, 5.66 mmol) and 4-(4-aminophenyl)-butyric acid (1.05 mg, 5.66 mmol) were added. The mixture was stirred at 140°C under argon atmosphere for 24 h. After cooling, the crude product was poured over an ice/water mixture, filtered, washed with cold water several times and, finally, purified twice by flash chromatography ( $\text{SiO}_2$ ,  $\text{CH}_2\text{Cl}_2 \rightarrow \text{CH}_2\text{Cl}_2/\text{acetone}$  10:1), to yield an orange solid (1.2 g, 25% yield).  $^1\text{H}$  NMR (300 MHz,  $\text{CDCl}_3$ , 25°C, TMS):  $\delta$ =8.77 (s, 2H; 2×H-PBI), 8.75 (s, 2H; 2×H-PBI), 7.53 (t,  $J$ =7.8 Hz, 1H; H-Ar), 7.43 (d,  $J$ =8.3 Hz, 2H; 2×H-Ar'), 7.37 (d,  $J$ =7.8 Hz, 2H; 2×H-Ar), 7.25 (d,  $J$ =8.3 Hz, 2H; 2×H-Ar'), 2.87–2.66 (m, 4H; Ar- $\text{CH}_2$  + 2×CH-(CH<sub>3</sub>)<sub>2</sub>), 2.49 (t,  $J$ =7.30 Hz, 2H;  $\text{CH}_2\text{-CO}_2\text{H}$ ), 2.16–2.01 (m, 2H; Ar- $\text{CH}_2\text{-CH}_2\text{-CH}_2\text{-CO}_2\text{H}$ ), 1.23–1.15 ppm (m, 12H; 4×CH<sub>3</sub>);  $^{13}\text{C}$  NMR (75 MHz,  $\text{CDCl}_3$ , 25°C, TMS):  $\delta$ =178.1, 162.5, 162.3, 145.6, 142.4, 135.6, 135.5, 133.4, 133.3, 132.4, 131.7, 131.6, 130.0, 129.9, 129.7, 128.9, 128.8, 128.4, 124.3, 123.9, 123.7, 123.5, 123.2, 34.8, 33.2, 29.3, 26.0, 24.0, ppm; IR (KBr):  $\tilde{\nu}$ =2957, 2928, 2096 (N<sub>3</sub>), 1704 (C=O imide), 1665 (C=O imide), 1588, 1493, 1434, 1392, 1368, 1349, 1286, 1236, 1172, 911, 805, 748, 686, 547 cm<sup>-1</sup>; UV/Vis ( $\text{CH}_2\text{Cl}_2$ ):  $\lambda_{\max}$  (log  $\epsilon$ )=232 (4.83), 278 (4.44), 426 (4.05), 486 (4.45), 519 nm (4.61); MS (MALDI-TOF):  $m/z$ : 721 [ $M]^+$  and 722 [ $M+H]^+$ ; elemental analysis calcd (%) for  $C_{35}H_{27}Cl_4N_3O_4 \cdot 1/2H_2O$ : C 57.31, H 3.85, N 9.55; found C 57.35, H 3.71, N 9.67.

**(PBI)<sub>2</sub>-SiPc 2:** SiPcCl<sub>2</sub> (50 mg, 0.082 mmol) and PBI 5 (278 mg, 0.33 mmol) in dyglyme (3 mL) were stirred at 160°C under argon atmosphere for 12 h. After cooling, the crude product was poured over water, filtered, washed with water several times and, finally, purified by flash chromatography ( $\text{SiO}_2$ ,  $\text{CH}_2\text{Cl}_2/\text{acetone}$  20:1→ $\text{CH}_2\text{Cl}_2/\text{acetone}/\text{MeOH}$  9:1:0.2) to yield a dark green solid (27 mg, 15% yield).  $^1\text{H}$  NMR (300 MHz,  $\text{CDCl}_3$ , 25°C, TMS):  $\delta$ =9.76–9.69 (m, 8H; 8×H-Pc), 8.77 (s, 4H; 4×H-PBI), 8.72 (s, 4H; 4×H-PBI), 8.43–8.37 (m, 8H; 8×H-Pc), 7.54 (t,  $J$ =7.9 Hz, 2H; 2×H-Ar'), 7.34 (d,  $J$ =7.9 Hz, 4H; 4×H-Ar'), 6.81 (d,  $J$ =8.3 Hz, 4H; 4×H-Ar), 6.31 (d,  $J$ =8.3 Hz, 4H; 2×H-Ar), 2.75 (m, 4H; 4×CH-(CH<sub>3</sub>)<sub>2</sub>), 1.24–1.13 (m, 24H, 8×CH<sub>3</sub>), 0.88 (t,  $J$ =7.2 Hz, 4H; 2×Ar-CH<sub>2</sub>), -0.34 to -0.54 ppm (m, 8H, 2×CH<sub>2</sub>-CH<sub>2</sub>-CO<sub>2</sub>H);  $^{13}\text{C}$  NMR (75 MHz,  $\text{CDCl}_3$ , 25°C, TMS):  $\delta$ =166.8, 162.4, 162.3, 150.1, 145.6, 142.0, 135.6, 135.7, 135.6, 135.5, 133.4, 133.2, 131.7, 131.6, 134.5, 131.4, 130.1, 129.8, 128.9, 128.8, 128.7, 127.6, 124.3, 124.1, 123.9, 123.6, 123.5, 123.2, 33.8, 33.0, 29.3, 24.3, 24.0 ppm; IR (KBr):  $\tilde{\nu}$ =2960, 2926, 1715 (C=O acid), 1678 (C=O imide) 1588, 1431, 1381, 1337, 1314, 1292, 1240, 1190, 1123, 1082, 914, 805, 737, 687, 546 cm<sup>-1</sup>; UV/Vis ( $\text{CH}_2\text{Cl}_2$ ):  $\lambda_{\max}$  (log  $\epsilon$ )=231 (5.28), 269 (4.93), 360 (4.85), 426 (4.38), 487 (4.80), 520 (4.95), 616 (4.56), 654 (4.49), 685 nm (5.26); HRMS (MALDI-TOF):  $m/z$ : calcd for  $C_{124}H_{78}Cl_8N_{12}O_{12}Si$ : 2234.3165 [ $M]^+$ ; found: 2234.3134; elemental analysis calcd (%) for  $C_{124}H_{78}Cl_8N_{12}O_{12}Si \cdot 4H_2O$ : C 64.50, H 3.90, N 7.22; found C 63.14, H 3.93, N 7.02.

**SiPc 6:** SiPcCl<sub>2</sub> (100 mg, 0.16 mmol) and 5-hexynoic acid (1.02 g, 9.06 mmol) in dyglyme (2 mL) were stirred at 160°C under argon atmosphere for 6 h. After cooling, the crude product was poured over water, filtered, washed with water several times and, finally, purified by flash chromatography ( $\text{SiO}_2$ ,  $\text{CH}_2\text{Cl}_2$ ) to yield a dark blue solid (39 mg 31% yield).  $^1\text{H}$  NMR (300 MHz,  $\text{CDCl}_3$ , 25°C, TMS):  $\delta$ =9.75–9.65 (m, 8H; 8×H-Pc), 8.42–8.34 (m, 8H; 8×H-Pc), 1.18 (t,  $J$ =2.7 Hz, 2H; 2×C≡C-H), 0.49–0.42 (m, 4H; 2×CH<sub>2</sub>-C≡C-H), -0.53–(-0.61) ppm (m, 8H; 2×CH<sub>2</sub>-CH<sub>2</sub>-CO<sub>2</sub>H);  $^{13}\text{C}$  NMR (75 MHz,  $\text{CDCl}_3$ , 25°C, TMS):  $\delta$ =166.3, 150.0, 135.6, 131.3, 124.0, 82.5, 67.7, 32.8, 21.7, 16.1 ppm; IR (KBr):  $\tilde{\nu}$ =3304 (C≡C-H), 2964, 1680, 1528, 1474, 1426, 1351, 1336, 1288, 1236, 1161, 1122, 1081, 1059, 914, 762, 732, 664, 536 cm<sup>-1</sup>; UV/Vis ( $\text{CH}_2\text{Cl}_2$ ):  $\lambda_{\max}$  (log  $\epsilon$ )=360 (4.87), 615 (4.59), 653 (4.52), 684 nm (5.35); MS (MALDI-TOF):  $m/z$ : 762 [ $M]^+$ ; elemental analysis calcd (%) for  $C_{44}H_{30}N_8O_4Si \cdot 1/2H_2O$ : C 68.38, H 4.04, N 14.50; found C 68.39, H 4.02, N 14.61.

**PBI derivative 7:** 1,6,7,12-Tetrachloroperylene-3,4:9,10-tetracarboxylic anhydride (2 g, 3.77 mmol), 3-azidopropylamine (517 mg, 4 mmol), 2-ethylhexylamine (517 mg, 4 mmol) and 25 mL of dry toluene, were stirred at 110°C under argon atmosphere for 24 h. After cooling, the solvent was evaporated and the crude product was purified twice by flash chromatography ( $\text{SiO}_2$ ,  $\text{CH}_2\text{Cl}_2 \rightarrow \text{CH}_2\text{Cl}_2/\text{acetone}$  20:3) to yield an orange solid (950 mg, 35% yield).  $^1\text{H}$  NMR (300 MHz,  $\text{CDCl}_3$ , 25°C, TMS):  $\delta$ =8.69 (s, 2H, 2×H-PBI), 8.68 (s, 2H; 2×H-PBI), 4.33 (t,  $J$ =7.1 Hz, 2H; N-CH<sub>2</sub>-CH<sub>2</sub>-CH<sub>2</sub>-N<sub>3</sub>), 4.23–4.08 (m, 2H; N-CH<sub>2</sub>-CH-R'), 3.47 (t,  $J$ =6.7 Hz, 2H; -CH<sub>2</sub>-N<sub>3</sub>), 2.66 (q,  $J$ =6.9 Hz, 2H; N-CH<sub>2</sub>-CH<sub>2</sub>-CH<sub>2</sub>-N<sub>3</sub>), 2.00–1.88 (m, 1H; -CH<sub>2</sub>-), 1.49–1.22 (m, 8H; 4×-CH<sub>2</sub>-), 1.02–0.86 ppm (m, 6H; 2×CH<sub>3</sub>);  $^{13}\text{C}$  NMR (75 MHz,  $\text{CDCl}_3$ , 25°C, TMS):  $\delta$ =162.6, 162.3, 135.5, 135.3, 133.1, 133.0, 131.5, 131.4, 128.8, 128.5, 123.4, 123.3, 122.9, 49.4, 44.6, 38.4, 30.8, 30.7, 28.7, 28.6, 27.6, 24.0, 23.1, 14.1, 10.6 ppm; IR (KBr):  $\tilde{\nu}$ =2957, 2928, 2096 (N<sub>3</sub>), 1704 (C=O imide), 1665 (C=O imide), 1588, 1493, 1434, 1392, 1368, 1349, 1286, 1236, 1172, 911, 805, 748, 686, 547 cm<sup>-1</sup>; UV/Vis ( $\text{CH}_2\text{Cl}_2$ ):  $\lambda_{\max}$  (log  $\epsilon$ )=232 (4.83), 278 (4.44), 426 (4.05), 486 (4.45), 519 nm (4.61); MS (MALDI-TOF):  $m/z$ : 721 [ $M]^+$  and 722 [ $M+H]^+$ ; elemental analysis calcd (%) for  $C_{35}H_{27}Cl_4N_3O_4 \cdot 1/2H_2O$ : C 57.31, H 3.85, N 9.55; found C 57.35, H 3.71, N 9.67.

**(PBI)<sub>2</sub>-SiPc 3:** SiPc 6 (15 mg, 0.02 mmol) and PBI 7 (32 mg, 0.04 mmol) were suspended in a 4:1 THF/H<sub>2</sub>O mixture (5 mL), and treated with CuSO<sub>4</sub>·5H<sub>2</sub>O (5% mol, 0.54 mg, 0.002 mmol) and sodium ascorbate (10% mol, 0.85 mg, 0.004 mmol). The mixture was stirred at 60°C for 24 h. After cooling, the solvent was evaporated and the crude product was purified by flash chromatography ( $\text{SiO}_2$ ,  $\text{CH}_2\text{Cl}_2/\text{acetone}$  20:2→ $\text{CH}_2\text{Cl}_2/\text{acetone}$  20:3) to yield a dark green solid (35 mg, 80% yield).  $^1\text{H}$  NMR (300 MHz,  $\text{CDCl}_3$ , 25°C, TMS):  $\delta$ =9.72–9.63 (m, 8H; 8×H-Pc), 8.69 (s, 4H; 4×H-PDI), 8.55 (s, 4H; 4×H-PDI), 8.40–8.30 (m, 8H; 8×H-Pc), 6.20 (s, 2H; 2×H-triazole), 4.22–4.06 (m, 12H; 6×N-CH<sub>2</sub>), 2.23–2.11 (m, 4H; 2×N-CH<sub>2</sub>-CH<sub>2</sub>), 2.03–1.90 (m, 2H; 2×CH), 1.49–1.20 (m, 16H; 8×CH<sub>2</sub>), 1.03–0.75 (m, 16H; 4×CH<sub>3</sub> + 2×CH<sub>2</sub>-triazole), -0.46 (m, 4H; 2×O<sub>2</sub>C-CH<sub>2</sub>-CH<sub>2</sub>), 0.61 ppm (t,  $J$ =7.5 Hz, 4H; 2×O<sub>2</sub>C-CH<sub>2</sub>-CH<sub>2</sub>);  $^{13}\text{C}$  NMR (75 MHz,  $\text{CDCl}_3$ , 25°C, TMS):  $\delta$ =166.7, 162.6, 162.1, 150.0, 146.4, 135.6, 135.5, 135.3, 133.0, 132.9, 131.5, 131.3, 128.8, 128.4, 124.0, 123.3, 123.2, 123.1, 122.7, 120.0, 47.7, 44.6, 38.0, 33.1, 30.7, 28.6, 28.4, 24.0, 23.9, 23.1, 23.0, 22.5, 14.1, 10.6 ppm; IR (KBr):  $\tilde{\nu}$ =2955, 2928, 1705 (C=O imide), 1666 (C=O imide), 1589, 1432, 1391, 1337, 1288, 1237, 1165, 1123, 1082, 914, 805, 738, 686, 546 cm<sup>-1</sup>; UV/Vis ( $\text{CH}_2\text{Cl}_2$ ):  $\lambda_{\max}$  (log  $\epsilon$ )=230 (5.28), 279 (4.88), 360 (4.87), 426 (4.37), 486 (4.74), 520 (4.90), 616 (4.56), 655 (4.49), 686 nm (5.35); HRMS (MALDI-TOF):  $m/z$ : calcd for  $C_{114}H_{84}Cl_8N_{18}O_{12}Si$ : 2204.3787 [ $M]^+$ ; found: 2204.3788; elemental analysis calcd (%) for  $C_{114}H_{84}Cl_8N_{18}O_{12}Si \cdot 2H_2O$ : C 60.97, H 3.95, N 11.23; found C 60.92, H 3.83, N 11.29.

**Laser flash photolysis:** A solution of ZnPc-PBI in MeCN was excited by a Panther OPO pumped by Nd:YAG laser (Continuum, SLII-10, 4–6 ns fwhm, 1.5 and 3.0 mJ pulse<sup>-1</sup>) at  $\lambda$ =531 nm. The transient absorption measurements were performed using a continuous xenon lamp (150 W) and an InGaAs-PIN photodiode (Hamamatsu 2949) as the probe light and detector, respectively. The output from the photodiodes and a photo-multiplier tube was recorded with a digitized oscilloscope (Tektronix, TDS3032, 300 MHz). Femtosecond transient absorption spectroscopy experiments were conducted using an ultrafast source (Integra-C, Quanttronix Corp.), an optical parametric amplifier (TOPAS, Light Conversion Ltd.) and a commercially available optical detection system (Helios, Ultrafast Systems LLC). The source for the pump and probe pulses were derived from the fundamental output of Integra-C (780 nm, 2 mJ pulse<sup>-1</sup> and fwhm=130 fs) at a repetition rate of 1 kHz. 75% of the fundamental output of the laser was introduced into TOPAS, which has optical frequency mixers, resulting in a tunable range from 285 to 1660 nm, while the rest of the output was used for white light generation. Typically, 2500 excitation pulses were averaged for 5 s to obtain the transient spectrum at a set delay time. Kinetic traces at appropriate wavelengths were assembled from the time-resolved spectral data. All measurements were conducted at 298 K. The transient spectra were recorded using fresh solutions in each laser excitation.

For nanosecond laser flash photolysis experiments, deaerated solutions of the dyad were excited by a Panther OPO equipped with a Nd:YAG laser

(Continuum, SLII-10, 4–6 ns fwhm) at  $\lambda=430$  nm with the power of 10 mJ pulse<sup>-1</sup>. The photochemical reactions were monitored by continuous exposure to a Xe-lamp (150 W) as a probe light and a photomultiplier tube (Hamamatsu 2949) as a detector. The transient spectra were recorded using fresh solutions for each laser excitation. The solution was deoxygenated by argon purging for 15 min prior to the measurements.

**Theoretical calculations:** Density-functional theory (DFT) calculations were performed on a COMPAQ DS20E computer. Geometry optimizations of (PBI)<sub>2</sub>-SiPc **1–3** were carried out using the Becke3LYP functional and 3-21G basis set,<sup>[25–27]</sup> with the restricted Hartree-Fock (RHF) formalism as implemented in the Gaussian 03 program Revision C.02. Graphical outputs of the computational results were generated with the Gauss View software program (ver. 3.09) developed by Semichem, Inc.

## Acknowledgements

This work was partially supported by Grants-in-Aid from the Ministry of Education, Culture, Sports, Science and Technology, Japan (Nos. 21750146 and 20108010), KOSEF/MEST through WCU project (R31-2008-000-10010-0), and by Grants from MICINN, FEDER, and Generalitat Valenciana (Consolider-Ingenio 2010 project HOPE CSD2007-00007, CTQ2007-67888/BQU, CTQ2008-05901/BQU, CTQ2010-20349, ACOMP/2009/039 and ACOMP/2009/056). F.J.C.-G. thanks the Spanish Government MICINN for a FPU fellowship. L.M.G. thanks the Global Education and Research Center for Bio-Environmental Chemistry of Osaka University for stage grants.

- [1] See, for example: a) L. Sánchez, M. Sierra, N. Martín, A. J. Myles, T. J. Dale, J. Rebek, Jr., W. Seitz, D. Guldi, *Angew. Chem.* **2006**, *118*, 4753–4757; *Angew. Chem. Int. Ed.* **2006**, *45*, 4637–4641; b) S. Fukuzumi, K. Ohkubo, *Coord. Chem. Rev.* **2010**, *254*, 372–385; c) S. Fukuzumi, *Phys. Chem. Chem. Phys.* **2008**, *10*, 2283–2297; d) A. Mateo-Alonso, C. Ehli, D. Guldi, M. Prato, *J. Am. Chem. Soc.* **2008**, *130*, 14938–14939; e) K. A. Nielsen, G. H. Sarova, L. Martín-Gomis, F. Fernández-Lázaro, P. C. Stein, L. Sanguinet, E. Levillain, J. L. Sessler, D. M. Guldi, Á. Sastre-Santos, J. O. Jeppesen, *J. Am. Chem. Soc.* **2008**, *130*, 460–462; f) F. D’Souza, R. Chitta, S. Gadde, L. M. Rogers, P. A. Karr, M. E. Zandler, A. S. D. Sandanayaka, Y. Araki, O. Ito, *Chem. Eur. J.* **2007**, *13*, 916–922; g) S. Fukuzumi, T. Kojima, *J. Mater. Chem.* **2008**, *18*, 1427–1439.
- [2] a) V. Balzani, A. Credi, M. Venturi, *ChemSusChem* **2008**, *1*, 26–58; b) S. Fukuzumi, *Eur. J. Inorg. Chem.* **2008**, 1351–1362.
- [3] a) V. Balzani, A. Credi, M. Venturi, *Chem. Eur. J.* **2008**, *14*, 26–39; b) H. Sakai, H. Murata, M. Murakami, K. Ohkubo, S. Fukuzumi, *Appl. Phys. Lett.* **2009**, *95*, 252901/1–3.
- [4] a) H. Imahori, H. Yamada, D. M. Guldi, Y. Endo, A. Shimomura, S. Kundu, K. Yamada, T. Okada, Y. Sakata, S. Fukuzumi, *Angew. Chem.* **2002**, *114*, 2450–2453; *Angew. Chem. Int. Ed.* **2002**, *41*, 2344–2347; b) S. Fukuzumi, T. Honda, K. Ohkubo, T. Kojima, *Dalton Trans.* **2009**, 3880–3889.
- [5] a) K. D. Jordan, M. N. Paddon-Row, *Chem. Rev.* **1992**, *92*, 395–410; b) F. D. Lewis, R. L. Letsinger, M. R. Wasielewski, *Acc. Chem. Res.* **2001**, *34*, 159–170; c) M. A. Smitha, E. Prasad, K. R. Gopidas, *J. Am. Chem. Soc.* **2001**, *123*, 1159–1165; d) H. Imahori, D. M. Guldi, K. Tamaki, Y. Yoshida, C. Luo, Y. Sakata, S. Fukuzumi, *J. Am. Chem. Soc.* **2001**, *123*, 6617–6628.
- [6] a) B. Albinsson, M. P. Eng, K. Pettersson, M. U. Winters, *Phys. Chem. Chem. Phys.* **2007**, *9*, 5847–5864; b) T. Honda, T. Nakanishi, K. Ohkubo, T. Kojima, S. Fukuzumi, *J. Am. Chem. Soc.* **2010**, *132*, 10155–10156.
- [7] a) N. R. Lokan, M. N. Paddon-Row, M. Koeberg, J. W. Verhoeven, *J. Am. Chem. Soc.* **2000**, *122*, 5075–5081; b) M. Fujitsuka, N. Tsuboya, R. Hamasaki, M. Ito, S. Onodera, O. Ito, Y. Yamamoto, *J. Phys. Chem. A* **2003**, *107*, 1452–1458; c) S. Fukuzumi, K. Ohkubo, W. E. Z. Ou, J. Shao, K. M. Kadish, J. A. Hutchison, K. P. Ghiggino, P. J. Santic, M. J. Crossley, *J. Am. Chem. Soc.* **2003**, *125*, 14984–14985.

- [8] a) P. Samori, X. Yin, N. Tchebotareva, Z. Wang, T. Pakula, F. Jäckel, M. D. Watson, A. Venturini, K. Müllen, J. P. Rabe, *J. Am. Chem. Soc.* **2004**, *126*, 3567–3575; b) M. J. Ahrens, L. E. Sinks, B. Rybtchinski, W. Liu, B. A. Jones, J. M. Giaimo, A. V. Gusev, A. J. Goshe, D. M. Tiede, M. R. Wasielewski, *J. Am. Chem. Soc.* **2004**, *126*, 8284–8294; c) F. Würthner, Z. Chen, F. J. M. Hoeben, P. Osswald, C-C. You, P. Jonkheijm, J. V. Herrikhuyzen, A. P. H. J. Schenning, P. P. A. M. van der Schoot, E. W. Meijer, E. H. A. Beckers, S. C. J. Meskers, R. A. J. Janssen, *J. Am. Chem. Soc.* **2004**, *126*, 10611–10618; d) X. Li, L. E. Sinks, B. Rybtchinski, M. R. Wasielewski, *J. Am. Chem. Soc.* **2004**, *126*, 10810–10811; e) B. Rybtchinski, L. E. Sinks, M. R. Wasielewski, *J. Am. Chem. Soc.* **2004**, *126*, 12268–12269; f) E. H. A. Beckers, S. C. J. Meskers, A. P. H. J. Schenning, Z. Chen, F. Würthner, P. Marsal, D. Beljonne, J. Cornil, R. A. J. Janssen, *J. Am. Chem. Soc.* **2006**, *128*, 649–657.
- [9] a) K. Ohkubo, J. Ortiz, L. Martín-Gomis, F. Fernández-Lázaro, A. Sastre-Santos, S. Fukuzumi, *Chem. Commun.* **2007**, 589–591; b) L. Martín-Gomis, K. Ohkubo, F. Fernández-Lázaro, S. Fukuzumi, A. Sastre-Santos, *Org. Lett.* **2007**, *9*, 3441–3444.
- [10] a) F. Würthner, *Chem. Commun.* **2004**, 1564–1579; b) H. Langhals, *Helv. Chim. Acta* **2005**, *88*, 1309–1343.
- [11] a) S. Fukuzumi, K. Ohkubo, J. Ortiz, A. M. Gutierrez, F. Fernández-Lázaro, A. Sastre-Santos, *Chem. Commun.* **2005**, 3814–3816; b) S. Fukuzumi, K. Ohkubo, J. Ortiz, A. M. Gutierrez, F. Fernández-Lázaro, A. Sastre-Santos, *J. Phys. Chem. A* **2008**, *112*, 10744–10752; c) F. J. Céspedes-Guirao, K. Ohkubo, S. Fukuzumi, Á. Sastre-Santos, F. Fernández-Lázaro, *J. Org. Chem.* **2009**, *74*, 5871–5880; d) M. Planells, F. J. Céspedes-Guirao, A. Forneli, Á. Sastre-Santos, F. Fernández-Lázaro, E. Palomares, *J. Mater. Chem.* **2008**, *18*, 5802–5808; e) M. Planells, F. J. Céspedes-Guirao, L. Gonçalves, Á. Sastre-Santos, F. Fernández-Lázaro, E. Palomares, *J. Mater. Chem.* **2009**, *19*, 5818–5825; f) R. D. Costa, F. J. Céspedes-Guirao, H. J. Bolink, J. Gierschner, E. Ortí, F. Fernández-Lázaro, Á. Sastre-Santos, *Chem. Commun.* **2009**, 3886–3888; g) R. D. Costa, F. J. Céspedes-Guirao, H. J. Bolink, F. Fernández-Lázaro, Á. Sastre-Santos, E. Ortí, J. Gierschner, *J. Phys. Chem. C* **2010**, *114*, 19192–19297.
- [12] a) G. de La Torre, C. G. Claessens, T. Torres, *Chem. Commun.* **2007**, 2000–2015; b) *Phthalocyanine Materials: Synthesis Structure and Function* (Ed.: N. B. McKeown), Cambridge University Press, Cambridge, **1998**; c) *Phthalocyanines-Properties and Applications*, Vol. 1 (Eds.: C. C. Leznoff, A. B. P. Lever), VCH, Weinheim, **1989**; *Phthalocyanines-Properties and Applications*, Vol. 2–3 (Eds.: C. C. Leznoff, A. B. P. Lever), VCH, Weinheim, **1993**; *Phthalocyanines-Properties and Applications*, Vol. 4 (Eds.: C. C. Leznoff, A. B. P. Lever), VCH, Weinheim, **1996**.
- [13] a) F. Gallego-Gómez, J. A. Quintana, J. M. Villalvilla, M. A. Díaz-García, L. Martín-Gomis, F. Fernández-Lázaro, Á. Sastre-Santos, *Chem. Mater.* **2009**, *21*, 2714–2720; b) F. J. Céspedes-Guirao, L. Martín-Gomis, F. Fernández-Lázaro, Á. Sastre-Santos, *J. Porphyrins Phthalocyanines* **2009**, *13*, 266–274; c) A. Sastre, A. Gouloumis, P. Vázquez, T. Torres, V. Doan, B. J. Schwartz, F. Wudl, L. Echegoyen, J. Rivera, *Org. Lett.* **1999**, *1*, 1807–1810; d) S.-G. Liu, A. Gouloumis, A. Sastre, P. Vázquez, T. Torres, L. Echegoyen, *Chem. Eur. J.* **2000**, *6*, 3600–3607.
- [14] a) M. Zhang, T. Murakami, K. Ajima, K. Tsuchida, A. S. D. Sandanayaka, O. Ito, S. Iijima, M. Yudasaka, *Proc. Natl. Acad. Sci. USA* **2008**, *105*, 14773–14778; b) M. Sibrian-Vazquez, J. Ortiz, I. V. Nesterova, F. Fernández-Lázaro, Á. Sastre-Santos, S. A. Soper, M. G. H. Vicente, *Bioconjugate Chem.* **2007**, *18*, 410–420.
- [15] a) L. de La Garza, R. van Grondelle, D. Gust, T. A. Moore, A. L. Moore, J. T. M. Kennis, *J. Phys. Chem. B* **2004**, *108*, 414–425; b) J. L. Rodríguez-Redondo, Á. Sastre-Santos, F. Fernández-Lázaro, D. Soares, G. C. Azzellini, B. Elliott, L. Echegoyen, *Chem. Commun.* **2006**, 1265–1267; c) S. Dayal, R. Krolicki, Y. Lou, X. Qiu, J. C. Berlin, M. E. Kenney, C. Burda, *Appl. Phys. B* **2006**, *84*, 309–315; d) M. E. El-Khouly, E. S. Kang, K.-Y. Kay, C. S. Choi, Y. Araki, O. Ito, *Chem. Eur. J.* **2007**, *13*, 2854–2863; e) L. Martin-Gomis, K. Ohkubo, F. Fernández-Lázaro, S. Fukuzumi, Á. Sastre-Santos, *J. Phys. Chem. C* **2008**, *112*, 17694–17701; f) J.-Y. Liu, E. A. Ermilov,

- B. Röder, D. K. P. Ng, *Chem. Commun.* **2009**, 1517–1519; g) M. E. El-Khouly, J. H. Kim, K.-Y. Kay, C. S. Choi, O. Ito, S. Fukuzumi, *Chem. Eur. J.* **2009**, *15*, 5301–5310; h) L. Martin-Gomis, K. Ohkubo, F. Fernandez-Lazaro, S. Fukuzumi, Á. Sastre-Santos, *Chem. Commun.* **2010**, *46*, 3944–3946.
- [16] N. B. McKeown, *J. Mater. Chem.* **2000**, *10*, 1979–1995.
- [17] a) J. D. Miller, E. D. Baron, H. Scull, A. Hsia, J. C. Berlin, T. McConnick, V. Colussi, M. E. Kenney, K. D. Cooper, N. L. Oleinick, *Toxicol. Appl. Pharmacol.* **2007**, *224*, 290–299; b) Y. Cheng, A. C. Samia, J. Li, M. E. Kenney, A. Resnick, C. Burda, *Langmuir* **2010**, *26*, 2248–2255; c) X.-J. Jiang, P.-C. Lo, Y.-M. Tsang, S.-L. Yeung, W.-P. Fong, D. K. P. Ng, *Chem. Eur. J.* **2010**, *16*, 4777–4783.
- [18] S. Honda, H. Ohkita, H. Benten, S. Ito, *Chem. Commun.* **2010**, *46*, 6596–6598.
- [19] M. S. Rodríguez-Morgade, T. Torres, C. Atienza-Castellanos, D. M. Guldi, *J. Am. Chem. Soc.* **2006**, *128*, 15145–15154.
- [20] a) R. F. Kelley, W. S. Shin, B. Rybtchinski, L. E. Sinks, M. R. Wasilewski, *J. Am. Chem. Soc.* **2007**, *129*, 3173–3181; b) Á. J. Jiménez, F. Spänić, M. S. Rodríguez-Morgade, K. Ohkubo, S. Fukuzumi, D. M. Guldi, T. Torres, *Org. Lett.* **2007**, *9*, 2481–2484.
- [21] C. Kohl, J. Qu, K. Müllen, WO 2004/076563A1, **2004**.
- [22] M. J. S. Dewar, E. G. Zoebisch, E. F. Healy, J. J. P. Stewart, *J. Am. Chem. Soc.* **1985**, *107*, 3902–3909.
- [23] J. Silver, J. L. Sosa-Sánchez, C. S. Frampton, *Inorg. Chem.* **1998**, *37*, 411–417.
- [24] W. E. Ford, P. V. Kamat, *J. Phys. Chem.* **1987**, *91*, 6373–6380.
- [25] A. D. Becke, *J. Chem. Phys.* **1993**, *98*, 5648–5652.
- [26] Gaussian 03, Revision C.02, M. J. Frisch, G. W. Trucks, H. B. Schlegel, G. E. Scuseria, M. A. Robb, J. R. Cheeseman, J. A. Montgomery, J. T. Vreven, K. N. Kudin, J. C. Burant, J. M. Millam, S. S. Iyengar, J. Tomasi, V. Barone, B. Mennucci, M. Cossi, G. Scalmani, N. Rega, G. A. Petersson, H. Nakatsuji, M. Hada, M. Ehara, K. Toyota, R. Fukuda, J. Hasegawa, M. Ishida, T. Nakajima, Y. Honda, O. Kitao, H. Nakai, M. Klene, X. Li, J. E. Knox, H. P. Hratchian, J. B. Cross, C. Adamo, J. Jaramillo, R. Gomperts, R. E. Stratmann, O. Yazyev, A. J. Austin, R. Cammi, C. Pomelli, J. W. Ochterski, P. Y. Ayala, K. Morokuma, G. A. Voth, P. Salvador, J. J. Dannenberg, V. G. Zakrzewski, S. Dapprich, A. D. Daniels, M. C. Strain, O. Farkas, D. K. Malick, A. D. Rabuck, K. Raghavachari, F. B. Foresman, J. V. Ortiz, Q. Cui, A. G. Baboul, S. Clifford, J. Ciosowski, B. B. Stefanov, G. Liu, A. Liashenko, P. Piskorz, I. Komaromi, R. L. Martin, D. J. Fox, T. Keith, M. A. Al-Laham, C. Y. Peng, A. Nanayakkara, M. Challacombe, P. M. W. Gill, B. Johnson, W. Chen, M. W. Wong, C. Gonzalez, J. A. Pople. Gaussian, Inc., Wallingford CT, **2004**.
- [27] R. Dennington II, T. Keith, J. Millam, K. Eppinnett, W. L. Hovell, R. Gilliland, Semichem, Inc., Shawnee Mission, KS, **2003**.

Received: January 28, 2011

Published online: June 28, 2011